SUPPLEMENTAL FIGURES

Figure S1

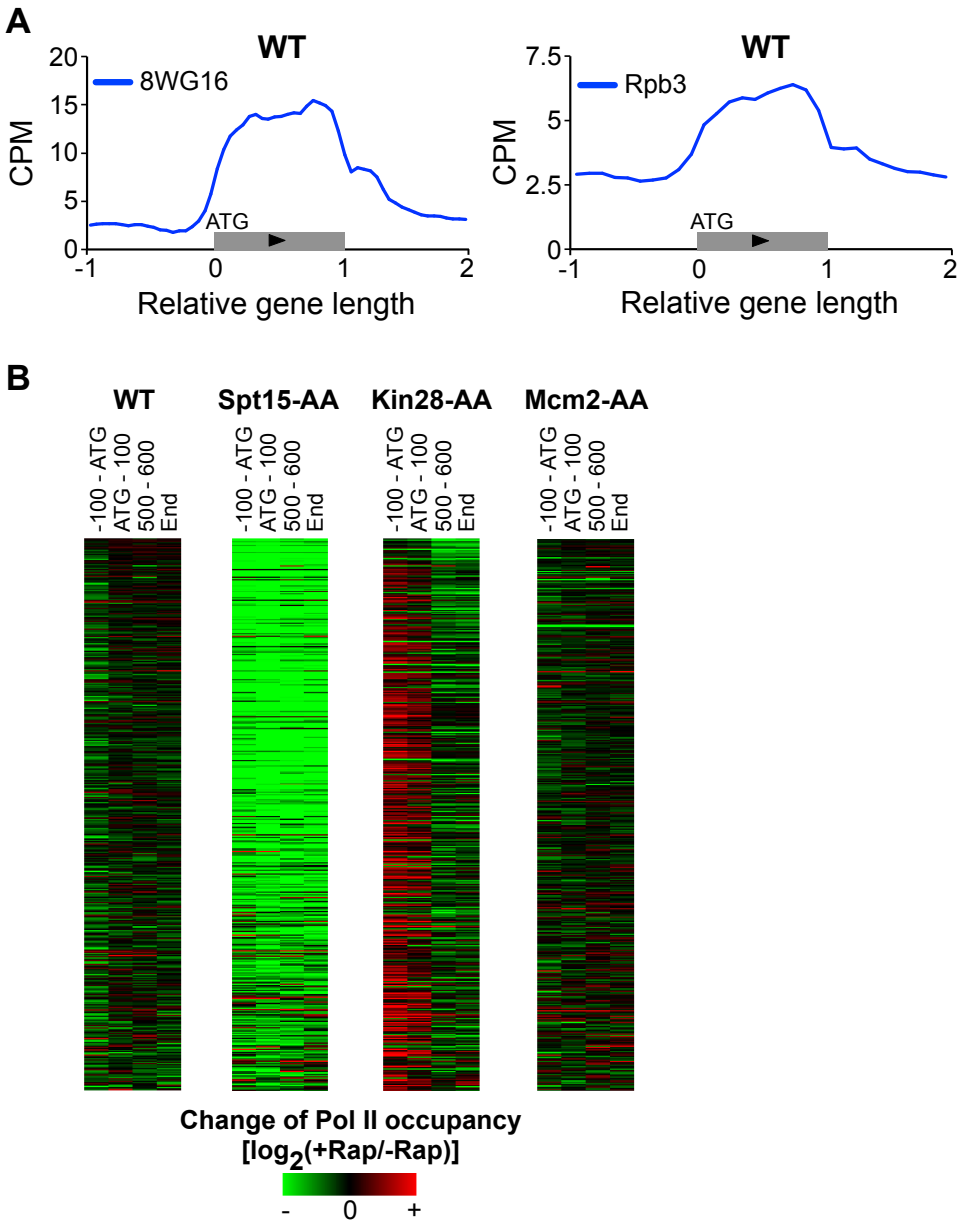

Figure S2

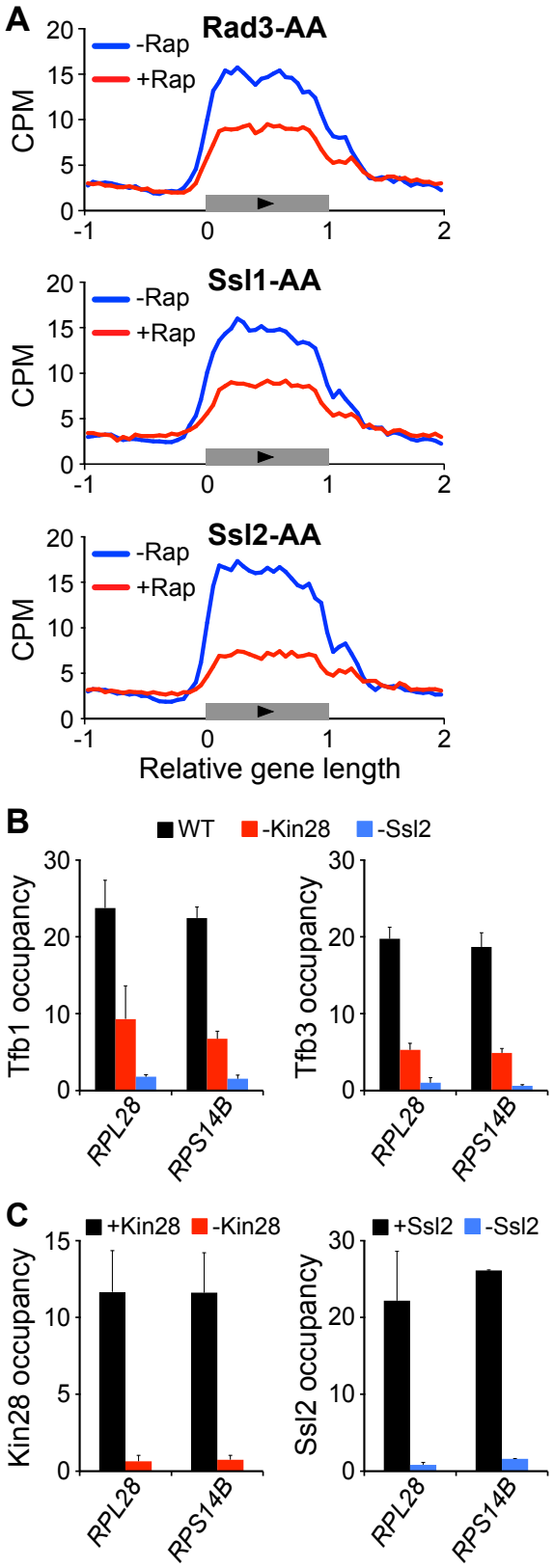
A
Rad3-AA
-Rap
+Rap
CPM
Ssl1-AA
Ssl2-AA
Relative gene length
B
WT
-Kin28
-Ssl2
Tfb1 occupancy
Tfb3 occupancy
RPL28
RPS14B
C
+Kin28
-Kin28
+Ssl2
-Ssl2
Kin28 occupancy
Ssl2 occupancy

Figure S3

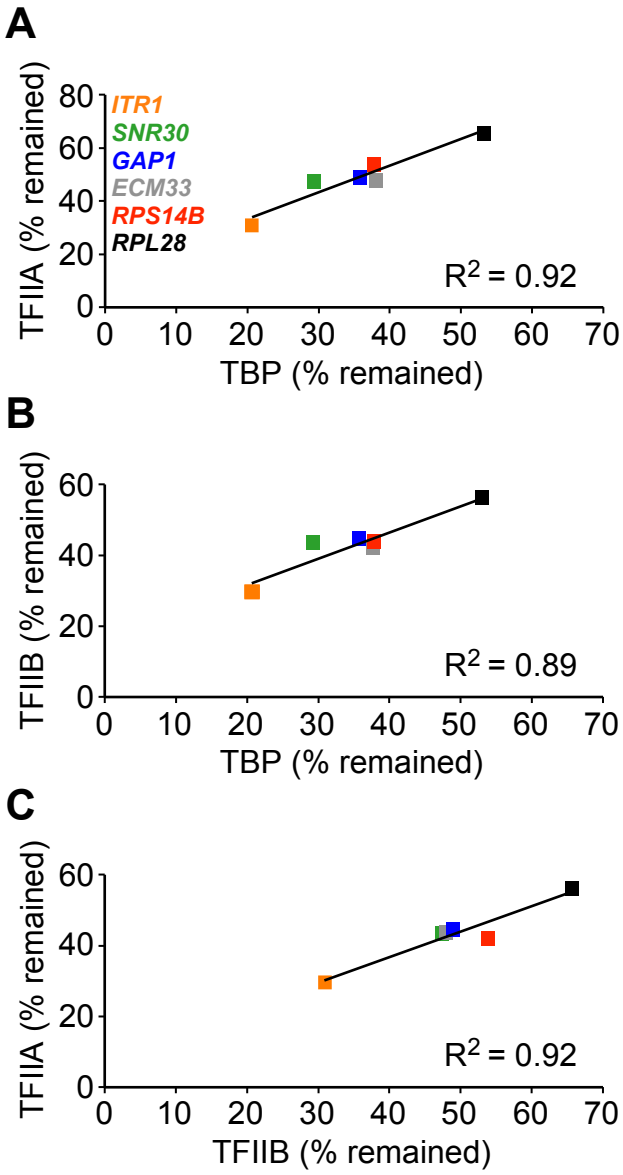
A
ITR1
SNR30
GAP1
ECM33
RPS14B
RPL28
TFIIA (% remained)
TBP (% remained)
R2 = 0.92
B
TFIIB (% remained)
TBP (% remained)
R2 = 0.89
C
TFIIA (% remained)
TFIIB (% remained)
R2 = 0.92

Figure S4

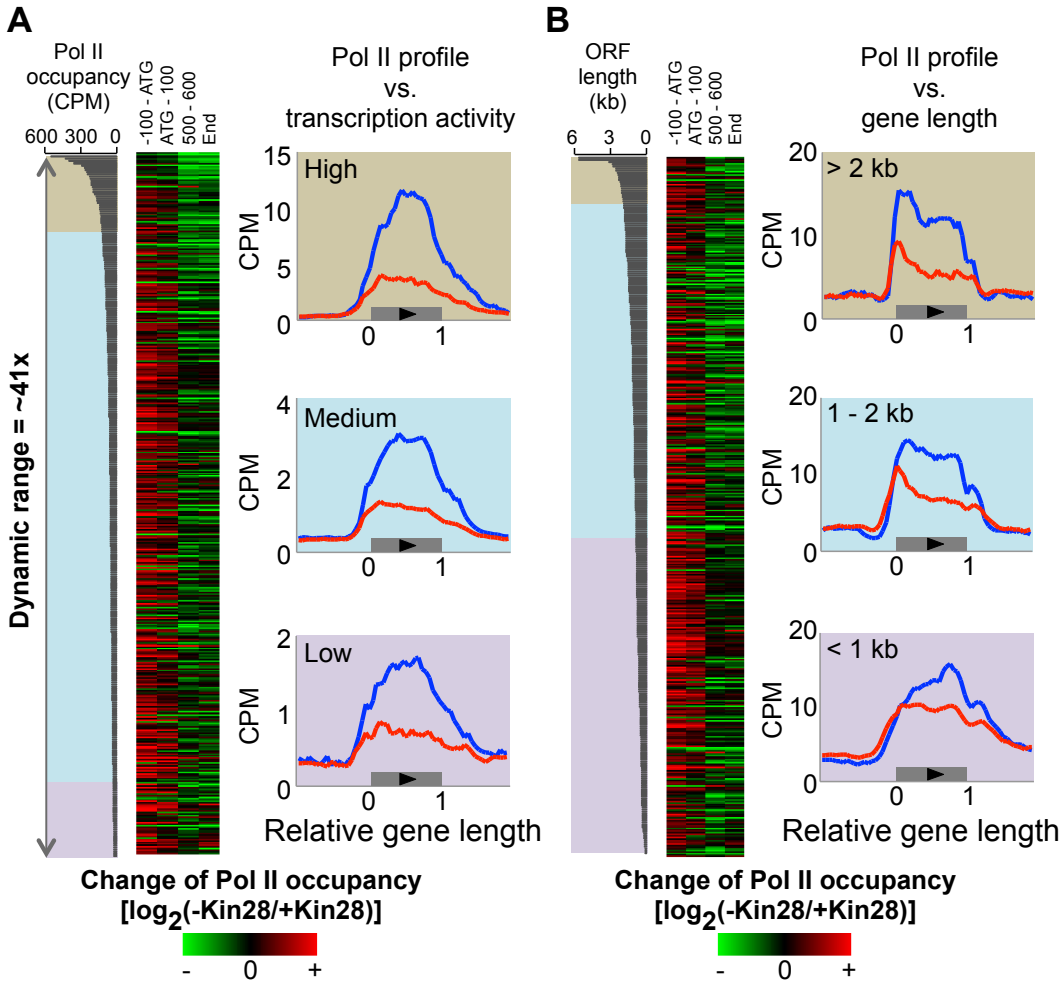
A
Pol II occupancy (CPM)
600 300 0
-100 - ATG
ATG - 100
500 - 600
End
Dynamic range = ~41x
Pol II profile vs. transcription activity
High
Medium
Low
CPM
Relative gene length
Change of Pol II occupancy [log2(-Kin28/+Kin28)]
- 0 +
B
ORF length (kb)
6 3 0
Pol II profile vs. gene length
> 2 kb
1 - 2 kb
< 1 kb
CPM
Relative gene length
Change of Pol II occupancy [log2(-Kin28/+Kin28)]
- 0 +

Figure S5

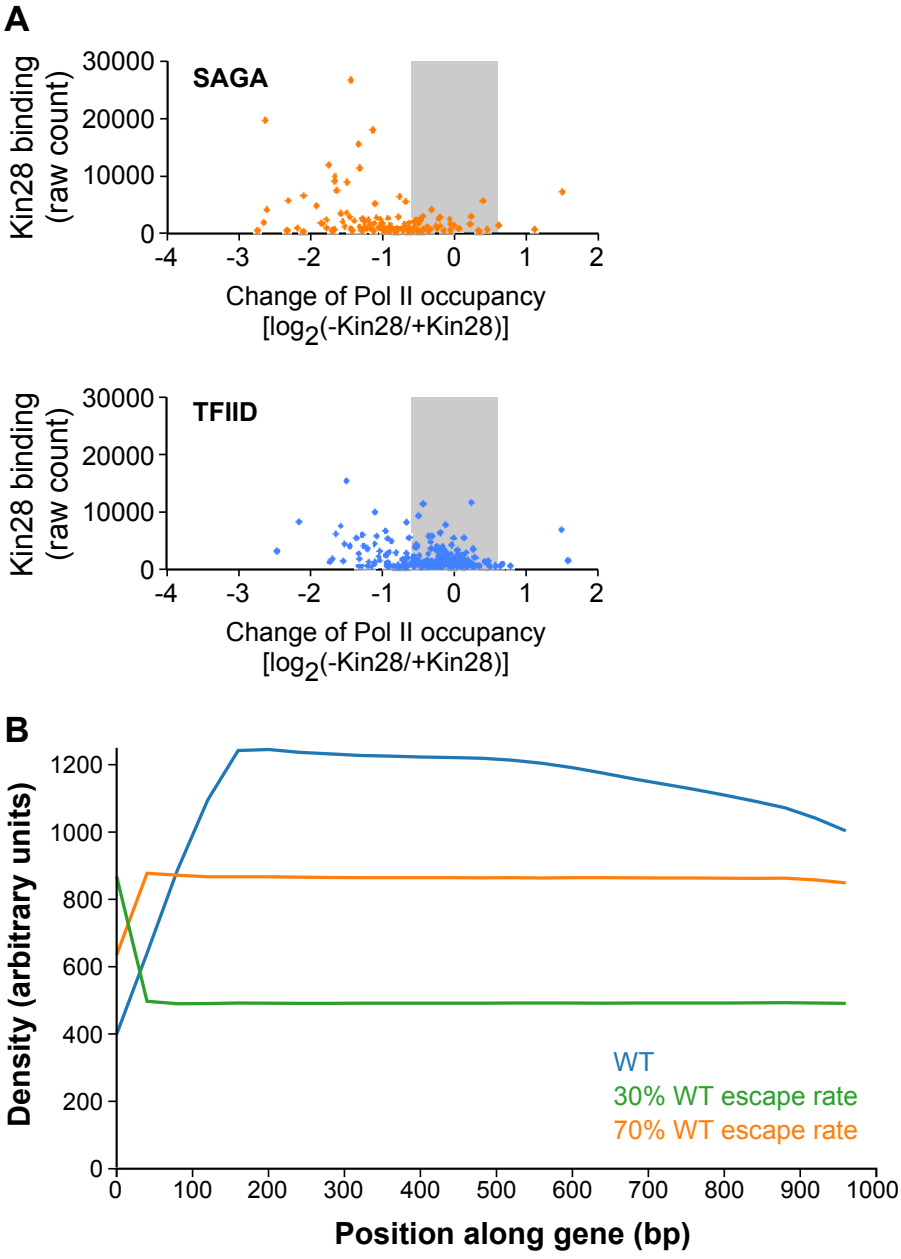
A
SAGA
Kin28 binding (raw count)
30000
20000
10000
0
-4
-3
-2
-1
0
1
2
Change of Pol II occupancy
[log2(-Kin28/+Kin28)]
TFIID
Kin28 binding (raw count)
Change of Pol II occupancy
[log2(-Kin28/+Kin28)]
B
Density (arbitrary units)
1200
1000
800
600
400
200
0
100
200
300
400
500
600
700
800
900
1000
Position along gene (bp)
WT
30% WT escape rate
70% WT escape rate

Figure S6

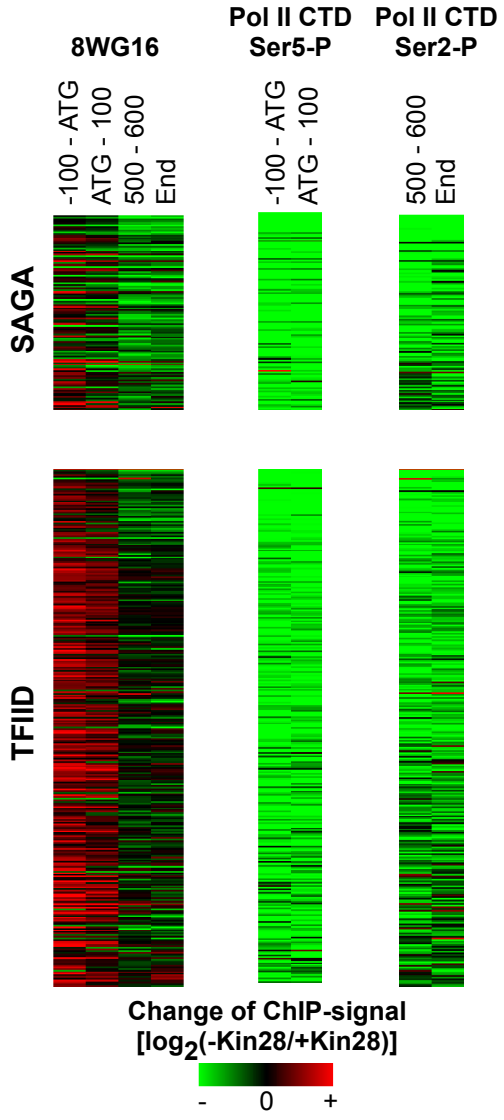
8WG16
Pol II CTD Ser5-P
Pol II CTD Ser2-P
-100 - ATG
ATG - 100
500 - 600
End
-100 - ATG
ATG - 100
500 - 600
End
SAGA
TFIID
Change of ChIP-signal
[log2(-Kin28/+Kin28)]
-
0
+

Figure S7

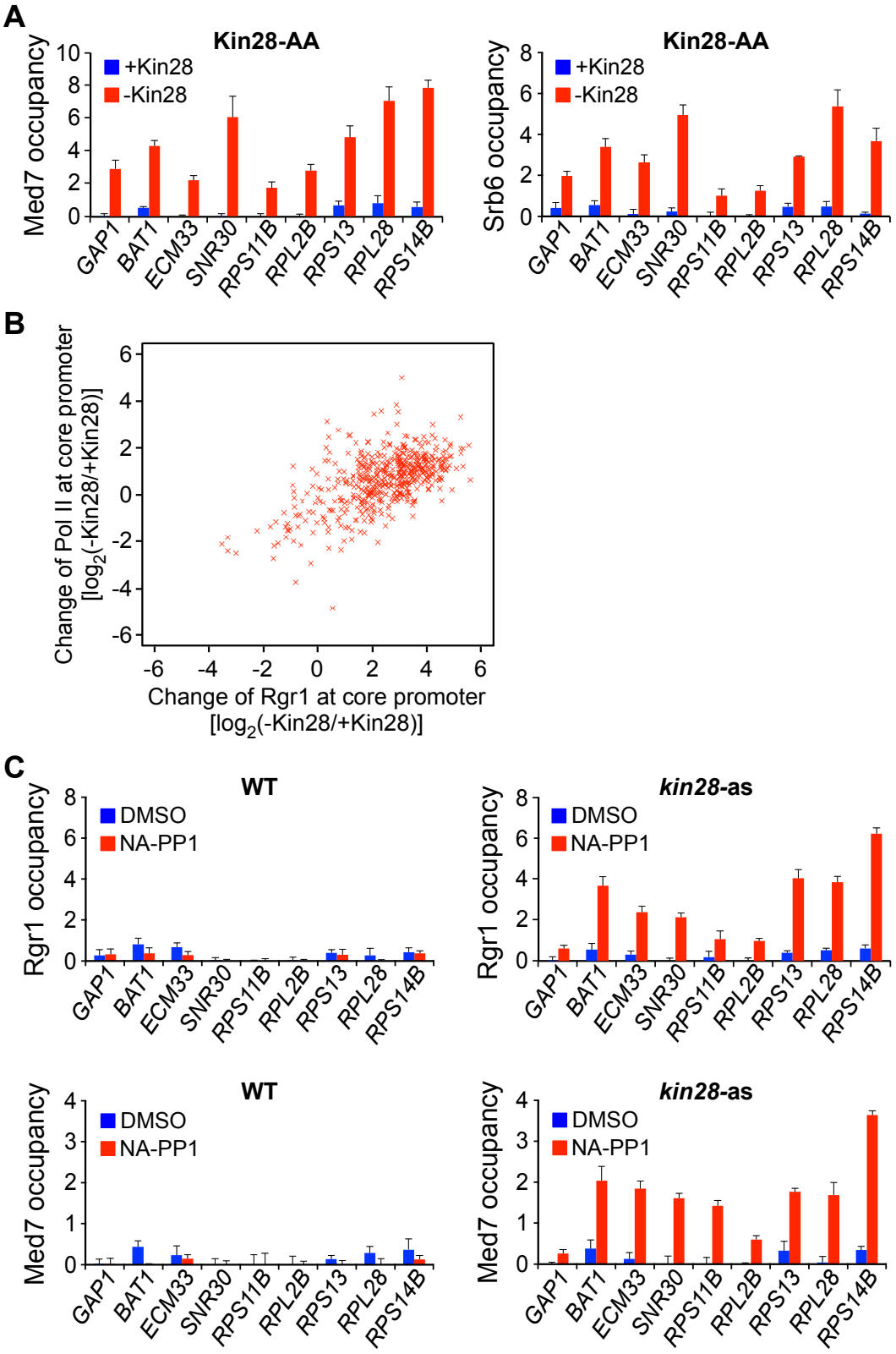
A
Kin28-AA
+Kin28
-Kin28
Med7 occupancy
Srb6 occupancy
GAP1
BAT1
ECM33
SNR30
RPS11B
RPL2B
RPS13
RPL28
RPS14B
B
Change of Pol II at core promoter
[log2(-Kin28/+Kin28)]
Change of Rgr1 at core promoter
[log2(-Kin28/+Kin28)]
C
WT
kin28-as
DMSO
NA-PP1
Rgr1 occupancy
Med7 occupancy

SUPPLEMENTAL FIGURE LEGENDS

Figure S1, related to Figure 1

Transcription effect in the Kin28 anchor-away strain upon rapamycin treatment

(A) Pol II ChIP-seq profiles of Rpb3 and un-phosphorylated CTD of Rpb1 are highly comparable. Overall Pol II ChIP-seq binding profiles of active genes were measured by antibodies against Rpb3 or un-phosphorylated CTD of Rpb1 (8WG16). Coding region of each gene was divided into 20 bins and reads were averaged for each bin within the range. For each bin, the median read count over all active genes was computed, normalized to the overall number of mapped reads, and plotted as counts per million mapped reads (CPM).

(B) Heat maps showing the Pol II occupancy changes at the indicated regions of active genes in WT, Spt15-AA, Kin28-AA and Mcm2-AA strains after 1-hour rapamycin treatment.

Figure S2, related to Figure 2

Effects of depletion of the TFIIH subunit Rad3, Ssl1, Ssl2, or Kin28

(A) Depletion of the TFIIH subunit Rad3, Ssl1, or Ssl2 causes general reduction in Pol II occupancy throughout coding regions without causing Pol II re-distribution to 5' ends of genes. Overall Pol II ChIP-seq binding profiles of active genes in the Rad3-AA, Ssl1-AA and Ssl2-AA strains before and after 1 hour of rapamycin treatment were plotted as in Figure S1A.

(B) TFIIH subunits Tfb1 and Tfb3 occupancies at the core promoters of indicated genes in the Kin28-AA and Ssl2-AA strains upon 1-hour rapamycin treatment.

(C) Kin28-FRB occupancy at the core promoters of indicated genes in the Kin28-AA strain before and after Kin28 depletion. Ssl2-FRB occupancy at the core promoters of indicated genes in the Ssl2-AA strain before and after Ssl2 depletion.

Averages and standard errors of three individual experiments are presented.

Figure S3, related to Figure 3

Kin28 depletion affects PIC formation

(A) Comparison between TFIIA and TBP occupancies at the core promoters of analyzed genes in the Kin28-AA strain upon Kin28 depletion. Percentage of occupancies remained after the rapamycin treatment was calculated and plotted.

(B) Comparison between TFIIB and TBP occupancies at the core promoters of analyzed genes in the Kin28-AA strain upon Kin28 depletion.

(C) Comparison between TFIIA and TFIIB occupancies at the core promoters of analyzed genes in the Kin28-AA strain upon Kin28 depletion.

Figure S4, related to Figure 4

Kin28 effects are not correlated with transcription activities and gene lengths

(A) Genes are sorted by transcription activities (i.e. Pol II levels) on coding regions and are classified as having high (top 10%, gray shade), medium (intermediate between top and bottom 10%, blue shade) or low (bottom 10%, purple shade) transcription activity.

(B) Genes are sorted by their lengths (ORF length) and grouped into three classes; > 2 kb (gray shade), 1-2 kb (blue shade), and < 1 kb (purple shade).

Changes of Pol II occupancy at the indicated regions of active genes in the Kin28-AA strain upon Kin28 depletion are presented as $\log_2$ ratios of Pol II levels before and after rapamycin treatment in the heat maps. Overall Pol II ChIP-seq binding profile is also presented for each class of genes.

Figure S5, related to Figure 5

Kin28 depletion differentially affects SAGA- and TFIID-dependent genes

(A) The differential transcription effect between SAGA- and TFIID-dependent genes upon Kin28 depletion is not directly associated with the level of Kin28 binding at promoters. Transcription (as measured by Pol II occupancy at the 3' end of a gene) changes for SAGA-

and TFIID-dependent genes upon Kin28 depletion are plotted against promoter Kin28-FRB occupancies prior to its depletion. Promoter Kin28 occupancy was determined by the total count of Kin28 ChIP-seq reads within the 200 bp window immediate before the start codon (ATG) of coding region. Gray area indicates that the transcription effect is less than 2 folds.
(B) Pol II ChIP-seq profiles suggest differential promoter escape rates for SAGA- and TFIID-dependent genes in the absence of Kin28. Computational simulation of Pol II density profiles based on different promoter escape rates were generated using a previously published algorithm (Ehrensberger et al., 2013).

Figure S6, related to Figure 5

Phosphorylations of Ser5 and Ser2 residues of Rpb1 CTD are similarly affected by Kin28 depletion for SAGA- and TFIID-dependent genes

Heat maps present the changes of ChIP signals of unphosphorylated Pol II and phosphorylated Ser5 or Ser2 residue of Pol II CTD at the indicated regions of active SAGA- and TFIID-dependent genes after Kin28 depletion for 1 hour.

Figure S7, related to Figure 6

Kin28 depletion causes accumulation of Mediator at core promoters of active genes

(A) Mediator subunits Med7 and Srb6 occupancies at the core promoters of indicated genes in the Kin28-AA strain before and after Kin28 depletion. Averages and standard errors of three individual experiments are presented.
(B) Pol II and Mediator accumulations at core promoters are correlated. Pol II and Mediator (Rgr1) levels of each gene were measured by the total number of ChIP-seq reads within the 100 bp window immediately upstream of the translation start codon (ATG). The read counts were then normalized to the total number of mapped reads. Pol II and Mediator (Rgr1) occupancy changes were calculated and plotted as $\log_2$ ratios.

(C) Inactivation of Kin28 kinase activity causes accumulation of Mediator at core promoters of active genes. Mediator subunits Rgr1 and Med7 occupancies at the core promoters of indicated genes in the WT and *kin28*-as strains upon 1-hour treatment of the inhibitor NA-PP1 or DMSO. Result of Rgr1 occupancy in the *kin28*-as strain is identical to Figure 6E, reproduced here for comparison between WT and *kin28*-as strains. Averages and standard errors of three individual experiments are presented.

Table S1, related to Experimental Procedures

Yeast strains and primer sets used in this study are listed.

SUPPLEMENTAL REFERENCES

Ehrensberger, A.H., Kelly, G.P., and Svejstrup, J.Q. (2013). Mechanistic interpretation of promoter-proximal peaks and RNAPII density maps. Cell *154*, 713-715.